SIMULATION ON RING CURRENT FORMATION: A CASE STUDY OF A STORM ON FEBRUARY 13, 1972

Yusuke Ebihara[1], Masaki Ejiri[2] and Hiroshi Miyaoka[2]

[1] *Department of Polar Science, The Graduate University for Advanced Studies,*
Kaga 1-chome, Itabashi-ku, Tokyo 173-8515
[2] *National Institute of Polar Research, Kaga 1-chome, Itabashi-ku, Tokyo 173-8515*

Abstract: We developed a computer simulation scheme for the motion of energetic particles trapped in the Earth's magnetic field during a magnetic storm. The particles are injected into the inner magnetosphere from the near-Earth plasma sheet by a strong inductive electric field due to a dipolarization in association with a substorm. The motion of the particles is traced by the bounce-average approximation under a dipolar magnetic field and the Volland-Stern type convection field. The absolute quantity of a directional differential flux of the particles can be obtained. We can calculate the azimuthal component of the current density and an H-component of the magnetic disturbance at the center of the Earth (Dst^*) induced by the current. In this paper, we examine the formation of the ring current and the magnetic disturbance on the moderate storm occurred on February 13–14, 1972. We find that (1) the inductive electric field due to the dipolarization may be one of major contributors to Dst^* on this storm, (2) the steep variations of Dst^* in the main phase cannot reproduced by the inductive electric field model, (3) the intensity of Dst^* is sensitive to the number density in the near-Earth plasma sheet, that is, an enhancement of the number density in the near-Earth plasma sheet may produce the steep and the major variations of Dst^*.

1. Introduction

The terrestrial ring current develops drastically during a magnetic storm due to hot plasma injections from the near-Earth plasmasheet. The storm-time ring current usually decays within a few days. The characteristic negative excursion of the *Dst* index is regarded as a consequence of the enhancement of the ring current. Most of early studies of a magnetic storm dealt with the ring current as an equivalent wire current flowing westward that was estimated from the magnetic disturbances on the ground. However, as Akasofu and Chapman (1961) and Hoffman and Bracken (1965) initially pointed out, the actual ring current forms more complex structure, that is, an eastward current generally exists inside the westward current. The noticeable questions concerning the ring current dynamics are still remained; for example, how the ring current affects the *Dst* index, how substorm induction electric fields associated with dipolarization events affect ring current formation and what is the relationship between storms and substorms.

It is essential for the investigation of the ring current dynamics to trace energetic particles, which contribute to the ring current formation, because the motion of the energetic particles strongly depends on the geomagnetic activity. The motion of the energetic particles associated with a magnetic storm/substorm has been investigated by many authors (*e.g.*, Chen, 1970; McIlwain, 1974; Stern, 1975; Ejiri, 1978; Ejiri *et*

al., 1978). EJIRI (1978) examined the bounce-average drift trajectory of the newly injected particles associated with a storm/substorm under a dipolar magnetic field and the Volland-Stern type convection field (VOLLAND, 1973; STERN, 1975) with its intensity depending on *Kp* indices (MAYNARD and CHEN, 1975). LEE *et al.* (1983), WODNICKA (1989) and TAKAHASHI *et al.* (1990) investigated the evolution of the total number density of the newly injected particles by tracing single particle motion. However, they did not derive a differential flux. Recently, the method solving the kinetic equation of the phase space density has been introduced by FOK *et al.* (1993, 1995, 1996), JORDANOVA *et al.* (1994). Though their method to solve the kinetic equation is useful to derive the phase space density, the method cannot provide us with the small scale structure owing to the hydrodynamical treatment.

2. Model Description

2.1. Drift trajectory and flux calculation

We developed a computer simulation scheme for the energetic particles trapped in the Earth's magnetic field during a magnetic storm. The particles are injected into the inner magnetosphere from the near-Earth plasma sheet by a convection field and a strong inductive electric field due to a dipolarization associated with a substorm. The motion of the particles are traced by the bounce-average approximation under a dipolar magnetic field and the Volland-Stern type convection field (VOLLAND, 1973; STERN, 1975) with its intensity depending on *Kp* indices (MAYNARD and CHEN, 1975). The bounce-average drift velocity $\langle V_s \rangle$ is generally given by

$$\langle V_s \rangle = \frac{E \times B}{B^2} + \frac{2}{\tau_b} \int_{s_m}^{s'_m} \frac{T V_s}{v} ds, \tag{1}$$

$$V_s = \frac{mv^2}{qB^4} B \times (B \cdot \nabla)B + \frac{mv_\perp^2}{2qB^3} B \times \nabla B, \tag{2}$$

where E, B, τ_b, s_m, (s'_m), T, v, $v_\perp$, ds, m and q are an electric field, a magnetic field, a bounce period, conjugate mirror points, tensor for the coordinate conversion, a parallel velocity, a perpendicular velocity, a line element aligned with a field line, mass and charge, respectively (ROEDERER, 1970). The tensor T becomes the scalar $\cos^3 \lambda$ in the dipolar magnetic field, where λ is the latitude.

We can express the bounce-average drift velocity under the dipolar magnetic field as

$$\langle V_s \rangle = \frac{E \times B}{B^2} + \frac{WG(\alpha_0)}{qB^3} B \times \nabla B, \tag{3}$$

where W, α_0 and $G(\alpha_0)$ are energy, an equatorial pitch angle and a function of an equatorial pitch angle, respectively. We used an approximation formula of a function $G(\alpha_0)$ given by EJIRI (1978).

It is essential to calculate the absolute directional differential flux in order to derive the ring current. Following CLADIS and FRANCIS (1985), EBIHARA *et al.* (1998a) derived a method to calculate the absolute differential flux of the trapped particles traced by the bounce-average approximation. A packet particle including a number of real particles in the small phase space bin is injected from the night side boundary and is

traced by the bounce-average approximation. A directional differential flux on the equatorial plane j_0 (L, ϕ, W, y_0) where ϕ is MLT and $y_0 = \sin(\alpha_0)$ is obtained by summing the all real particles that enter a phase space bin $(\Delta L, \Delta \phi, \Delta W, \Delta y_0)$ fixed on the equatorial plane as

$$j_0 (L, \phi, W, y_0) = \frac{\sum N}{2\pi S \tau_b(y_0) y \Delta y \Delta W} , \qquad (4)$$

where S and N are the area of a virtual detector on the equatorial plane and the real number of particles, respectively. j_0 (L, ϕ, W, y_0) has a unit of $(1/\mathrm{m}^2 \, \mathrm{s} \, \mathrm{str} \, \mathrm{J})$ in the MKS unit. The off-equatorial flux j at a latitude of λ can be derived from the Liouville's theorem (ROEDERER, 1970) as

$$j(L, \phi, \lambda, W, y) = j_0(L, \phi, W, h(\lambda) y) , \qquad (5)$$

with

$$h(\lambda) \equiv \frac{\cos^3 \lambda}{(1 + 3 \sin^2 \lambda)^{1/4}} . \qquad (6)$$

2.2. Inductive electric field

Inductive electric fields due to the dipolarization associated with a substorm are often observed by satellites in the near-Earth plasma sheet. AGGSON et al. (1983) reported that the transient inductive field was observed at $L = 7.5$ with a time scale of 3 min and the intensity of $E_y = 15$ mV/m. We assume that the inductive field is a function of magnetic local time (MLT) ϕ, L-value and time t, and is expressed as

$$E_\phi = E_0 f_1(\phi) f_2(L) f_3(t) , \qquad (7)$$

where E_0, $f_1(\phi)$, $f_2(L)$ and $f_3(t)$ are a maximum intensity of the electric field, a normalized function of local time, L-value and time, respectively. The normalized functions $f_1(\phi)$, $f_2(L)$ and $f_3(t)$ are simply written here as

$$f_1(\phi) = \begin{cases} \left(1 - 10^{-\frac{\phi - \phi_1}{\Delta \phi}}\right) \cdot \left(1 - 10^{-\frac{\phi_2 - \phi}{\Delta \phi}}\right) & \text{for } \phi_1 \leq \phi \leq \phi_2 , \\ 0 & \text{for } \phi < \phi_1 \text{ or } \phi > \phi_2 , \end{cases} \qquad (8)$$

$$f_2(L) = \begin{cases} 1 - 10^{-\frac{L - L_1}{\Delta L}} & \text{for } L \geq L_1 , \\ 0 & \text{for } L < L_1 , \end{cases} \qquad (9)$$

$$f_3(t) = \exp\left(-\frac{(t - t_0)^2}{a}\right) , \qquad (10)$$

and

$$a = \frac{-(\Delta t/2)^2}{\log 0.1} , \qquad (11)$$

where ϕ_1 and ϕ_2 are the azimuthal boundary of the inductive field $(\phi_1 < \phi_2)$, L_1 is an inner edge of the field, Δt is a time scale of the field and $\Delta \phi$ and ΔL is a characteristic width of the boundary regions on the MLT and the L, respectively, and the functions are shown in Fig. 1. The onset time t_0 must be determined by ground or satellite observations.
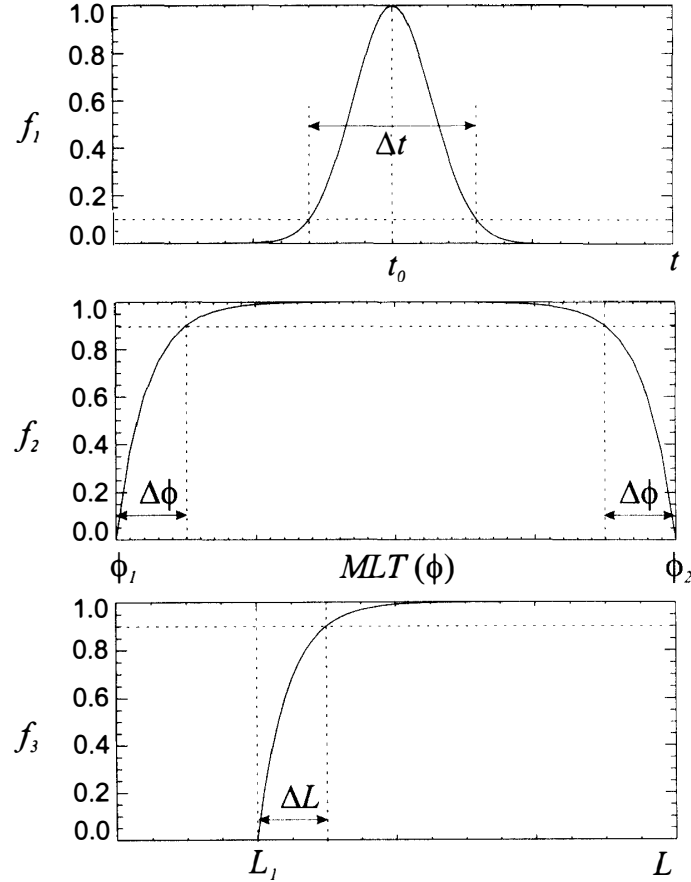
Fig. 1.   The inductive electric field model due to the dipolarization associated with the substorm. Functions f_1 (t), f_2 (φ) and f_3 (L) are corresponding to the eqs. (8) to (10), where t, φ and L are time, magnetic local time (MLT) and McIlwain's L-value, respectively.

2.3.   Loss processes of ions

We consider the two loss processes for the ions.   The first is the charge exchange with neutral hydrogens, and the second is the Coulomb collision with thermal electrons in the plasmasphere.   We use the charge exchange cross section derived from JANEV and SMITH (1993) and the Coulomb collision cross section derived from FOK et al. (1991). The neutral hydrogen density is derived from the spherically symmetric model of CHAMBERLAIN (1963).   The fitting parameter for the CHAMBERLAIN's (1963) model is given by RAIRDEN et al. (1986) based on the DE-1 observation.   Although the spatial distribution of the neutral hydrogen is relatively steady, the plasmasphere changes its form drastically depending on magnetospheric activity (e.g., CARPENTER, 1966; CHAPPELL, 1972).   We use the model of the plasmasphere described in EBIHARA et al. (1998b), which gives the three-dimensional electron density in fairly good agreement with the EXOS-B satellite observation.

3.   Results

In this paper, we investigate the moderate magnetic storm occurred on February 13, 1972, the minimum Dst being −47 nT.   The AL, Dst and Kp indices during the storm
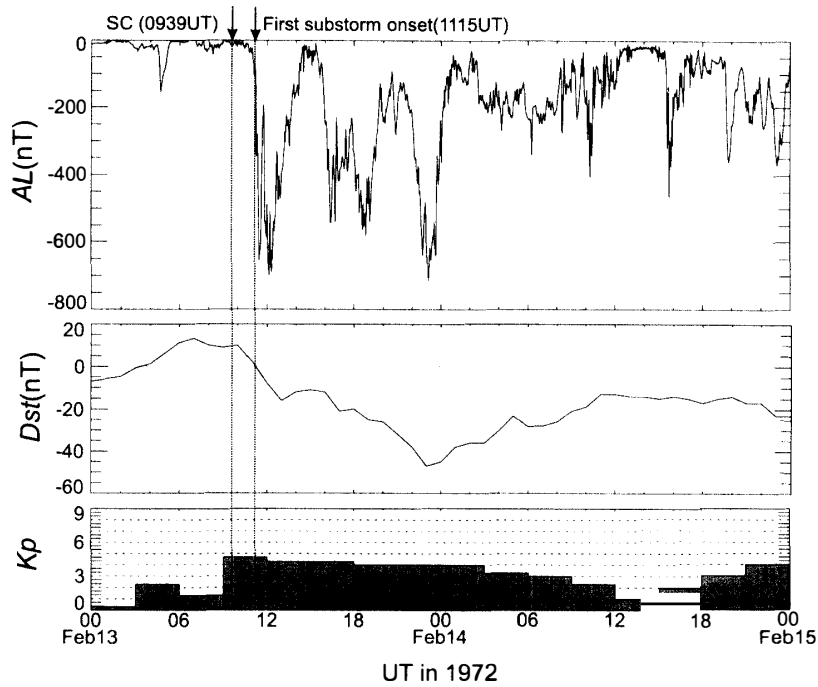
Fig. 2.   The AL, Dst and Kp indices on February 13-14, 1972.

are shown in Fig. 2.   There was a sudden commencement at 0939 UT, and the 13 substorms were identified by ground magnetograms during the main phase of this storm. The criterion that we identified onsets of the substorms is the beginning of a positive bay of the H-component magnetic disturbance with a time scale of ~ 1 hour recorded at a mid- or low-latitude station, except for the first substorm.   As for the first substorm onset, we identified it by the beginning of the sudden decrease of the magnetic field at the auroral zone.   In this period, the Explorer 45 satellite observed the successive directional differential fluxes of the ions and electrons with energy range of 0.8 keV to 870 keV for ions and 0.8 keV to 400 keV for electrons (LONGANECKER and HOFFMAN, 1973; SMITH and HOFFMAN, 1974; EJIRI et al., 1980).   After the first substorm onset occurred at 1115 UT, the Explorer 45 began to observe an enhancement of the ion flux at 1145 UT ($L=5$, MLT $=18.5$ h, near equatorial plane) with the characteristic energy dispersion (so-called nose structure).   EJIRI et al. (1978) numerically explained the energy dispersion of this event, that is, the dispersion in the E-t (energy-time) diagram is caused by the difference of the drift trajectories with time, depending on energy and the pitch angle of ions.   EBIHARA et al. (1998a) identified quantitatively the source distribution function and the temporal and spatial structure of the inductive electric field of this event; the source distribution function was isotropic Maxwellian with a temperature of 5 keV and a density of 0.22 cm^{3} at $L=8$ and the parameters for the model of the inductive electric field written in eqs. (7) to (11) were taken to be $E_0 = 10$ mV/m, $\phi_1 =$ 21 h, $\phi_2 = 3$ h(27 h), $\Delta\phi = 0.5$ h, $L_1 = 4.5$, $\Delta L = 1$, $\Delta t = 6$ min, respectively.   These values we identified on the first injection of the storm were apply to the later 12 injections.

We also inject electrons simultaneously with the ions.   The number density of the electrons is assumed to be equal to the ions owing to charge neutrality.   The satellite observations show statistically that ion and electron temperatures at the plasma sheet are

in the ratio of 2.6–7.3 at $L = 6.6$ (Thomsen *et al.*, 1996) and the ratio of ~ 7 at $L \sim 10$ -20 (Baumjohann, 1993). We assume the ratio of the temperature as 5 at $L = 8$.

3.1. Pressure and current density

The plasma pressure is given by

$$P_\perp = \int \frac{1}{2} f(v) m v^2 \sin^2 \alpha dv , \qquad (12)$$

$$P_\parallel = \int f(v) m v^2 \cos^2 \alpha dv , \qquad (13)$$

where f and v are a velocity distribution function and a velocity, respectively. We can rewrite eq. (12) and (13) as

$$P_\perp = \pi \sqrt{2m} \int_\alpha \int_W j_0(L, \phi, W, h(\lambda) \sin \alpha) \sqrt{W} \sin^3 \alpha d\alpha dW , \qquad (14)$$

$$P_\parallel = 2\pi \sqrt{2m} \int_\alpha \int_W j_0(L, \phi, W, h(\lambda) \sin \alpha) \sqrt{W} \cos^2 \alpha \sin \alpha d\alpha dW . \qquad (15)$$

The current density perpendicular to a field line (ring current) has been considered as a combination of the three currents; the magnetization current j_M, the curvature drift current j_R and the grad-B drift current j_B (Parker, 1957). The total current density $j_\perp$ is given by

$$\begin{aligned} j_\perp &= j_M + j_R + j_B \\ &= \frac{B}{B^2} \times \left[\nabla P_\perp + (P_\parallel - P_\perp) \frac{(B \cdot \nabla) B}{B^2} \right] . \end{aligned} \qquad (16)$$

In the dipolar magnetic field, the azimuthal component of the current density j_ϕ becomes

$$j_\phi = \frac{1}{B^2} \left(\frac{B_r}{r} \frac{\partial P_\perp}{\partial \lambda} - B_\lambda \frac{\partial P_\perp}{\partial r} \right) + \frac{1}{B^3} (P_\parallel - P_\perp) \left(\frac{B_r}{r} \frac{\partial B}{\partial \lambda} - B_\lambda \frac{\partial B}{\partial r} \right), \qquad (17)$$

$$= \frac{r^3}{M(1 + 3 \sin^2 \lambda)}$$

$$\left[-\frac{2}{r} \sin \lambda \frac{\partial P_\perp}{\partial \lambda} - \cos \lambda \frac{\partial P_\perp}{\partial r} + \frac{P_\parallel - P_\perp}{r} \left(-\frac{6 \sin^2 \lambda \cos \lambda}{1 + 3 \sin^2 \lambda} + 3 \cos \lambda \right) \right], \qquad (18)$$

where B_r, B_λ, r and M are the radial component of the magnetic field, the latitudinal component of the magnetic field, the radial distance from the center of the Earth, and the magnetic moment of the Earth, respectively.

The results of the calculation are shown in Fig. 3. We can see the bidirectional current flow; the borders of eastward and westward current flows are located at $L = 4.8$ (1210 UT, February 13) and $L = 4.4$ (0000 UT, February 14). The border was moved inward and the current density was enhanced as the storm developed. The current intensities reached peaks of 9.7 nA/m^2 for eastward current and 8.8 nA/m^2 for westward current, respectively at 0000 UT on February 14.

Lui *et al.* (1987) investigated the pressure and the current density by the AMPTE/ CCE satellite during the storm occurred on September 4, 1984. The current density reported by Lui *et al.* (1987) had peaks of 2.8 nA/m^2 ($L = 2.6$) for eastward current and 6.8 nA/m^2 ($L = 4.7$) for westward current, respectively, at the most disturbed time during the storm. The ratio of the current densities between the peaks was approximately 2.4. However, the calculated ratio was 0.91, that is, the calculated eastward
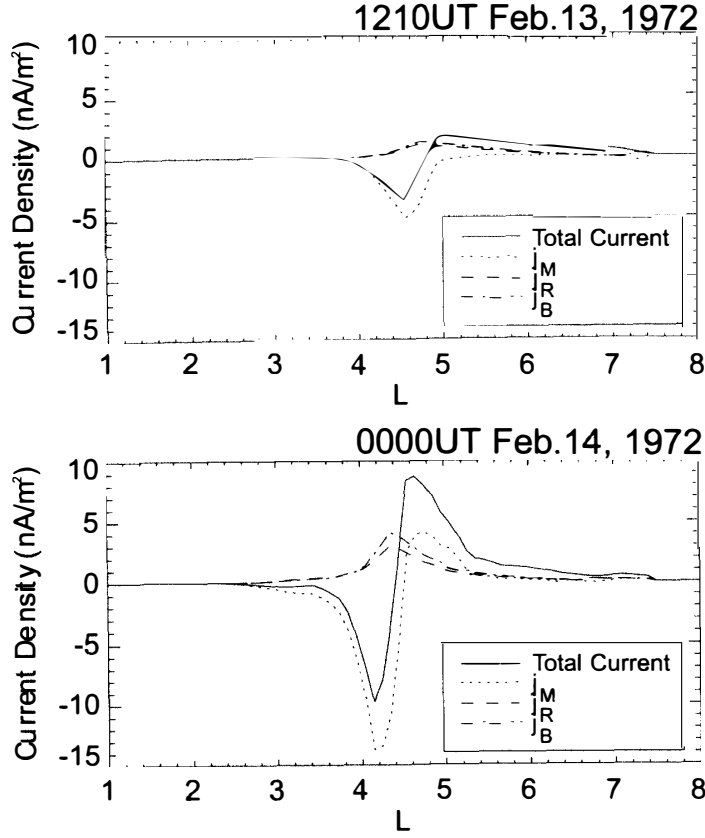
1210UT Feb.13, 1972

0000UT Feb.14, 1972

Fig. 3. *Cross sections of the equatorial current density j_ϕ in the midnight meridian at 1210 UT on February 13, 1972 (top panel) and 0000 UT on February 14 (bottom panel). Total current consists of the three currents, the magnetization current j_M (dotted line), the curvature drift current j_R (broken line) and the grad-B drift current j_B (dashed-dotted line). The positive quantity indicates the westward current.*

current was stronger than the westward one. The observational result showed that the pre-existing background pressure was responsible for the difference between the intensities of westward and east-ward currents. The background pressure had a peak at $L \sim 3$ for quiet time (LUI and HAMILTON, 1992). Since our model included no pre-existing background pressure, the westward current density was nearly equal to the eastward one. One possible origin of the background particles is the long-term transport due to the radial diffusion (*e.g.*, CHEN *et al.*, 1994).

3.2. Dst

An H-component magnetic disturbance at the center of the Earth ΔB can be calculated from the integration of the spatial distribution of the current density as

$$\Delta B = \int_r \int_\lambda \int_\phi \frac{\mu_0}{4\pi} \cos \lambda j_\phi(r, \lambda, \phi) \, dr d\lambda d\phi \,, \qquad (19)$$

where μ_0 is the permeability in vacuum. We regard ΔB as corrected Dst (hereafter Dst^*). Dst^* is given by subtracting the Chapman-Ferraro current from Dst, and is generally considered to be a good indicator of the strength of the ring current (*e.g.*, GONZALEZ *et al.*, 1994). A comparison between the calculated Dst^* and the observed one is shown in Fig. 4. The solid line in Fig. 4 is the calculated Dst^*, the source density
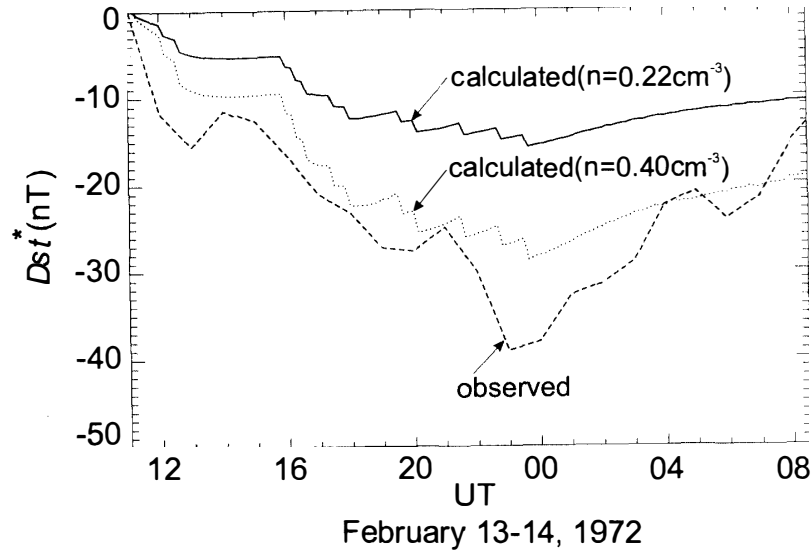
Fig. 4. A comparison between calculated Dst* and the observed Dst* of this storm on February 13–14, 1972. The source densities at the near-Earth plashasheet (L = 8) were taken to be 0.22 cm⁻³ (solid line) and 0.40 cm⁻³ (dotted line).

being 0.22 cm⁻³. Though the observed Dst^* (dashed line) reached to maximum of −39 nT, the calculated one reached to maximum of −16 nT. The dotted line is also calculated Dst^* but the source density is taken to be 0.40 cm⁻³. The dotted line is almost similar to the observed Dst^* except for steep variations around 1300 UT and 2300 UT on February 13, 1972. This result implies that the intensity of Dst^* is sensitive to the source density, and that the major contributor to the storm-time variation of Dst^* may be not only the inductive electric field due to the dipolarization but also the enhancement of the number density in the near-Earth plasmasheet. Therefore the steep variations around 1300 UT and 2300 UT may be produced by the enhancement of the number density in the near-Earth plasmasheet. For the large storm related to the magnetic cloud event, JORDANOVA et al. (1998) suggests that the superdense plasmasheet (BOROVSKY et al., 1997) mainly contributes to Dst^*. In general the number density in the near-Earth plasmasheet may play an important role in the intensity of Dst^* during a storm.

4. Summary and Conclusions

We traced the bounce-average trajectories of the newly injected particles during the magnetic storm and calculated the temporal evolution of the differential flux of the particles. The essential point of this model is to calculate the absolute quantity of the differential flux of the ring current particles. The plasma pressure and the azimuthal component of the current density were also calculated. Though the magnetic disturbance at the center of the Earth (Dst^*) was calculated with a formula between the total energy of the ring current and Dst^* (e.g., DESSLER and PARKER, 1959; SCKOPKE, 1966), we can calculate directly the Dst^* from the spatial distribution of the current density. The conclusions of our results are as follows.

1) The calculated eastward current density is stronger than the westward one at the most disturbed time of this storm. The ratio between them is 0.91. However, the

pre-existing background pressure having a peak at $L \sim 3$ is responsible for the difference between the intensities of westward and eastward currents because the observational result shows the ratio of 2.4 (LUI *et al.*, 1987).

2) The inductive electric field due to the dipolarization may be one of major contributors to Dst^* for this storm.

3) The intensity of Dst^* is sensitive to the number density in the near-Earth plasmasheet. The sudden enhancements of the number density in the near-Earth plasmasheet may produce the steep variations of Dst^* around 1300 UT and 2300 UT on February 13, 1972.

Acknowledgments

References

AGGSON, T. L., HEPPNER, J. P. and MAYNARD, N. C. (1983): Observations of large magnetospheric electric fields during the onset phase of a substorm. J. Geophys. Res., **88**, 3981–3990.

AKASOFU, S.-I. and CHAPMAN, S. (1961): The ring current, geomagnetic disturbance, and the Van Allen radiation belts. J. Geophys. Res., **66**, 1321–1350.

BAUMJOHANN, W. (1993): The near-earth plasma sheet: An AMPTE IRM perspective. Space Sci. Rev., **64**, 141–163.

BOROVSKY, J. E., THOMSEN, M. F. and McCOMAS, D. J. (1997): The superdense plasma sheet: Plasma-spheric origin, solar wind origin, or ionospheric origin? J. Geophys. Res., **102**, 22089–22097.

CARPENTER, D. L. (1966): Whistler studies of the plasmapause in the magnetosphere. 1. Temporal variations in the position of the knee and some evidence on plasma motions near the knee. J. Geophys. Res., **71**, 693–709.

CHAMBERLAIN, J. W. (1963): Planetary coronae and atmospheric evaporation. Planet. Space Sci., **11**, 901–960.

CHAPPELL, C. R. (1972): Recent satellite measurements of the morphology and dynamics of the plasma-sphere. Rev. Geophys. Space Phys., **10**, 951–979.

CHEN, A. J. (1970): Penetration of low-energy protons deep into the magnetosphere. J. Geophys. Res., **75**, 2458–2467.

CHEN, M. W., LYONS, L. R. and SCHULZ, M. (1994): Simulations of phase space distributions of storm time proton ring current. J. Geophys. Res., **99**, 5745–5759.

CLADIS, J. B. and FRANCIS, W. E. (1985): The polar ionosphere as a source of the storm time ring current. J. Geophys. Res., **90**, 3465–3473.

DESSLER, A. J. and PARKER, E. N. (1959): Hydrodynamic theory of geomagnetic storms. J. Geophys. Res., **64**, 2239–2252.

EBIHARA, Y., EJIRI, M. and MIYAOKA, H. (1998a): Enhancements of differential flux of energetic particles in the inner magnetosphere associated with a magnetic storm. Proc. NIPR Symp. Upper Atmos. Phys., **11**, 150–153.

EBIHARA, Y., EJIRI, M. and MIYAOKA, H. (1998b): Coulomb lifetime of the ring current ions with time varying plasmasphere. Earth Planets Space, **50**, 371–382.

EJIRI, M. (1978): Trajectory traces of charged particles in the magnetosphere. J. Geophys. Res., **83**, 4798–4810.

EJIRI, M., HOFFMAN, R. A. and SMITH, P. H. (1978): The convection electric field model for the magnetosphere based on Explorer 45 observations. J. Geophys. Res., **83**, 4811–4815.

EJIRI, M., HOFFMAN, R. A. and SMITH, P. H. (1980): Energetic particle penetrations into the inner magnetosphere. J. Geophys. Res., **85**, 653–663.

FOK, M. C., KOZYRA, J. U., NAGY, A. F. and CRAVENS, T. E. (1991): Lifetimes of ring current particles due to Coulomb collisions in the plasmasphere. J. Geophys. Res., **96**, 7861–7867.

FOK, M.-C., KOZYRA, J. U., NAGY, A. F., RASMUSSEN, C. E. and KHAZANOV, G. V. (1993): Decay of equatorial ring current ions and associated aeronomical consequences. J. Geophys. Res., **98**, 19381–19393.

FOK, M.-C., MOORE, T. E., KOZYRA, J. U., HO, G. C. and HAMILTON, D. C. (1995): Three-dimensional ring current decay model. J. Geophys. Res., **100**, 9619–9632.

FOK, M. C., MOORE, T. E. and GREENSPAN, M. E. (1996): Ring current development during storm main phase. J. Geophys. Res., **101**, 15311–15322.

GONZALEZ, W. D., JOSELYN, J. A., KAMIDE, Y., KROEHL, H. W., ROSTOKER, G., TSURUTANI, B. T. and VASYLIUNAS, V. M. (1994): What is a geomagnetic storm ? J. Geophys. Res., **99**, 5771–5792.

HOFFMAN, R. A. and BRACKEN, P. A. (1965): Magnetic effects of the quiet-time proton belt. J. Geophys. Res., **70**, 3541–3556.

JANEV, R. K. and SMITH, J. J. (1993): Cross sections for collision processes of hydrogen atoms with electrons, protons, and multiple-charged ions. Atomic and Plasma-Material Interaction Data for Fusion, IAEA, **4**, 78–79.

JORDANOVA, V. K., KOZYRA, J. U., KHAZANOV, G. V., NAGY, A. F., RASMUSSEN, C. E. and FOK, M.-C. (1994): A bounce-averaged kinetic model of the ring current ion population. Geophys. Res. Lett., **21**, 2785–2788.

JORDANOVA, V. K., FARRUGIA, C. J., JANOO, L., QUINN, J. M., TORBERT, R. B., OGILVIE, K. W., LEPPING, R. P., STEINBURG, J. T., McCOMAS, D. J. and BELIAN, R. D. (1998): October 1995 magnetic cloud and accompanying storm activity: Ring current evolution. J. Geophys. Res., **103**, 79–92.

LEE, L. C., Corrick, G. and AKASOFU, S.-I. (1983): On the ring current energy injection rate. Planet. Space Sci., **31**, 901–911.

LONGANECKER, G. W. and HOFFMAN, R. A. (1973): S3-A spacecraft and experiment description. J. Geophys. Res., **78**, 4711–4717.

LUI, A. T. Y. and HAMILTON, D. C. (1992): Radial profiles of quiet time magnetosphere parameters. J. Geophys. Res., **97**, 19325–19332.

LUI, A. T. Y., McENTIRE, R. W. and KRIMIGIS, S. M. (1987): Evolution of the ring current during two geomagnetic storms. J. Geophys. Res., **92**, 7459–7470.

MAYNARD, N. C. and CHEN, A. J. (1975): Isolated cold plasma regions: observations and their relation to possible production mechanisms. J. Geophys. Res., **80**, 1009–1013.

McILWAIN, C. E. (1974): Substorm injection boundaries. Magnetospheric Physics, ed. by B. M. McCORMAC. Dordrecht, D. Reidel, 143–154.

PARKER, E. N. (1957): Newtonian development of the dynamical properties of ionized gases of low density. Phys. Rev., **107**, 924–933.

RAIRDEN, R. L., FRANK, L. A. and CRAVEN, J. D. (1986): Geocoronal Imaging with Dynamics Explorer. J. Geophys. Res., **91**, 13613–13630.

ROEDERER, J. G. (1970): Dynamics of Geomagneticaly Trapped Radiation. Berlin, Springer.

SCKOPKE, N. (1966): A general relation between the energy of trapped particles and the disturbance field near the earth. J. Geophys. Res., **71**, 3125–3130.

SMITH, P. H. and HOFFMAN, R. A. (1974): Direct observation in the dusk hours of the characteristics of the storm time ring current particles during the beginning of magnetic storms. J. Geophys. Res., **79**, 966–967.

STERN, D. P. (1975): The motion of a proton in the equatorial magnetosphere. J. Geophys. Res., **80**, 595–599.

TAKAHASHI, S., IYEMORI, T. and TAKEDA, M. (1990): A simulation of the storm-time ring current. Planet. Space Sci., **38**, 1133–1141.

THOMSEN, M. F., BOROVSKY, J. E., McCOMAS, D. J. and MOLDWIN, M. B. (1996): Observations of the Earth's plasmasheet at geosynchronous orbit. Workshop on the Earth's Trapped Particle Environment, ed. by G. D. REEVES. New York, American Institute of Physics, 25–31.

VOLLAND, H. (1973): A semiempirical model of large-scale magnetospheric electric fields. J. Geophys. Res., **78**, 171–181.

WODNICKA, E. B. (1989): The magnetic storm main phase modeling. Planet. Space Sci., **37**, 525–534.